

Actuator Limitations on Achievable Manipulator Impedance

Dale A. Lawrence

Department of Electrical and Computer Engineering
University of Cincinnati, Cincinnati, OH 45221-0030

ABSTRACT

The effects of actuator torque/speed constraints on achievable manipulator mechanical impedance are discussed. Beginning with a simplified dynamic model, a describing function analysis is used to examine the constraints for linear behavior as well as the effective closed loop impedance resulting from the actuator nonlinear characteristic. It is shown that the closed loop manipulator impedance is a blend of two extreme impedances, and the degree of nonlinearity in the actuator controls the proportion of these two components in the overall dynamic response. The extension to multiple degree of freedom manipulators is also discussed, revealing behavioral properties similar to the single degree of freedom case. The relevance of this simple analysis to manipulator system preliminary design and feasibility studies is stressed.

INTRODUCTION

The objective of impedance control is to design and implement feedback control so that specific mechanical impedances are achieved at the manipulator end effector (or at any other location) [1]. Rather than controlling position or force directly, this objective places a constraint between position and force. Its chief advantage in accomplishing manipulation tasks is that interaction with external objects (e.g. task parts, other manipulators, etc.) is managed by "low level" servo control. This greatly reduces the detailed knowledge required at higher levels, and simplifies the planning and decision making required to perform basic motion functions [2,3].

While the common impedance control objective makes various implementations similar, they can be quite different in their achieved performance. Unmodeled system dynamics [4,5,6], actuator limitations [7,8], computation time delays [9], etc., can dominate the behavior of the closed loop system, causing poor performance—even instability. Therefore it is very important to identify, in the early stages of a design or feasibility study, those components of the system which most strongly limit the achievable performance.

This paper explores a common limitation in manipulation systems: actuator torque versus speed capabilities. The particular case of permanent magnet DC motor actuator technology is considered due to its widespread use and relatively simple torque/speed characteristic. Hydraulic actuators using servo valves have similar torque/speed constraints [8,15], and can also be studied with this approach. Using a model of the essential properties of a control loop containing an actuator of this type, results are derived for the closed loop nonlinear impedance of the manipulator, as well as for design and operational constraints under which linear impedances are retained. This data can be useful in the early stages of manipulator system design (both mechanical and control design) to determine the feasibility of achieving desired overall system impedances.

Compared to other work in characterizing the performance of manipulators, the results reported here are more comprehensive than the inertial characterizations [10,11,12], since the inertial behavior is only a part of the manipulator impedance. The characterization and design of manipulator compliance [21] is also a special case of the overall impedance. Control designs using actuator saturation have appeared using the optimal control approach [13] where minimum time criteria are involved. But they do not characterize the interaction behavior of the manipulator with its environment. The explicit use of actuator torque/speed constraints is used in simulation studies [7] to test whether actuator saturation occurs. This is most useful in a CAD setting [16], where various designs can be tried in simulation, and the design iterated on that basis. The approach taken here is fundamentally different, since it yields an analytical description of manipulator behavior. In addition to providing design guidelines for avoiding actuator saturation, this analysis also characterizes the effects of saturation when it does occur.

Section 1 introduces the model of the manipulator control loop, as well as the actuator torque/speed limitation considered. A describing function analysis of the effects of the actuator nonlinearity is presented in Section 2, and Section 3 shows how the analysis can be used in two important system design scenarios. The use of the simplified analysis and results is extended to treat more general manipulators in Section 4.

1. ONE DEGREE OF FREEDOM MODELING

This section will examine a simple model of manipulator dynamics, together with a typical actuator torque/speed constraint. The goal is a basic understanding of the effects of this nonlinear actuator characteristic on the closed loop manipulator impedance. Section 4 will discuss extensions of the single degree of freedom results to more complex situations.

Consider the following single degree of freedom system. A torque τ_m is applied to a single manipulator joint, with resulting joint angle θ . The joint dynamics are represented by the linear frequency domain function $Z_m(s)$.

$$\tau_m(s) = Z_m(s)\theta(s) \quad (1-1)$$

The function Z_m is termed the manipulator impedance; it describes the relationship between externally applied torques and resulting motions.

Since the manipulator impedance rarely represents acceptable dynamic behavior as it stands, feedback control is used to modify the impedance to a desired extent. If the feedback is represented in the form

$$\tau_a(s) = C(s)\theta(s) = (Z_m(s) - Z_c(s))\theta(s), \quad (1-2)$$

where τ_a is an actuator command torque, then the closed loop system has the form shown in Figure 1-1. The signal

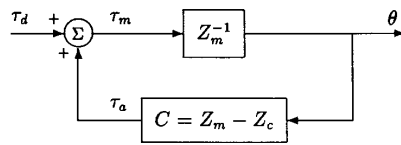


Figure 1-1: A general feedback loop for impedance control.

τ_d in Figure 1-1 is an external torque due to contact with the system's environment.

The closed loop transfer function from disturbance torque τ_d to the motion θ is the inverse of the controlled impedance Z , i.e.

$$\tau_d(s) = Z(s)\theta(s). \quad (1-3)$$

Observe that with (1-2) this overall impedance in Figure 1-1 is given by

$$\frac{\tau_d(s)}{\theta(s)} = \left[\frac{Z_m^{-1}(s)}{1 - C(s)/Z_m(s)} \right]^{-1} = Z_m(s) - C(s) = Z_c(s). \quad (1-4)$$

Thus in this linear case, the closed loop impedance is given by the Z_c term in the feedback control block.

In the case where the actuator cannot supply any desired torque at any speed, the linear description of the closed loop impedance given above will become nonlinear.

A description of this impedance will be provided for the case where the external torque is sinusoidal in form. While not a generic situation, it is a common one encountered in the dynamic analysis of a physical system using swept sine functions. Also it provides strong evidence for the behavior of a system to more general inputs if these inputs are decomposed into their sinusoidal harmonics. That is, a forcing function having significant energy at a frequency ω can be expected to reveal the same type of behavior exhibited by the "sinusoidal impedance" at that frequency. This is not a precise analysis, but it can provide valuable data for feasibility studies and preliminary design.

The use of a specific signal form in the analysis of nonlinear systems is termed the describing function method, and is well known [17,18]. For the sinusoidal describing function, the first harmonic of the nonlinear system output is compared to the sinusoidal input. The resulting shift in sinusoid magnitude and phase is taken as the describing function of the nonlinear block. The key assumption is that the input to the nonlinear block is harmonically pure. This assumption is often satisfied when the linear portion of the feedback system contains sufficient low-pass filtering to remove harmonics generated by the nonlinearity. The inertial behavior of the open loop system Z_m provides the needed filtering for the problem at hand.

The nonlinearity addressed here is the torque/speed constraint present in actuators using permanent magnet DC motors. The rotation of the motor generates a voltage (back EMF) which opposes the commanded voltage. When the rotation speed is high enough, the back EMF voltage equals the power amplifier supply voltage, and no additional acceleration torque is available. This constraint is illustrated in Figure 1-2. The constant τ_o is the so-called

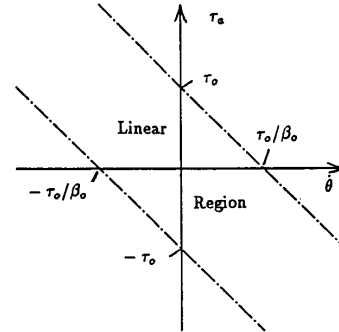


Figure 1-2: Actuator torque/speed constraint.

stall torque, and β_o is the back EMF constant. Inside these two linear constraints, the torque is determined by the linear control law $(C(s)/s)\dot{\theta}(s)$. (A current-type power amplifier is assumed here, where the motor current, hence its applied torque, is proportional to the command signal τ_a in this linear region.) Hydraulic actuators have similar constraints between delivered torque and speed, although the

characteristic is quadratic rather than linear [8,15]. When large torque is demanded by the control loop, either due to a large control gain or a large disturbance torque, the delivered torque τ_a becomes clipped or saturated, and “slides” along the constraint lines until the amplitude again lies in the linear region.

In the describing function analysis, the action of this torque/speed constraint is represented by a complex-valued function of frequency $D(j\omega)$, reflecting the magnitude and phase changes of the sinusoidal harmonics due to torque saturation. Thus, if the motion is $\theta(t) = a \sin(\omega t)$, the torque is $\tau_a(t) = a|D(j\omega)| \sin(\omega t + \angle D(j\omega))$, where $|\cdot|$ denotes the magnitude and \angle denotes the phase of the complex number $D(j\omega)$. In the frequency domain, this relation is written

$$\tau_a(j\omega) = D(j\omega)\theta(j\omega). \quad (1-5)$$

When saturation does not occur, the relation between τ_a and θ reduces to the transfer function $C(j\omega)$.

At each frequency ω the closed loop relation between the sinusoidal disturbance τ_d and the sinusoidal motion θ would be

$$\frac{\tau_d(j\omega)}{\theta(j\omega)} = \left[\frac{Z_m^{-1}(j\omega)}{1 - D(j\omega)/Z_m(j\omega)} \right]^{-1} = Z_m(j\omega) - D(j\omega) \quad (1-6)$$

as in the linear case before, only the controller C is now replaced with the actuator/controller describing function D . The next section discusses the properties of D using the torque/speed constraint of Figure 1-2.

2. THE TORQUE/SPEED DESCRIBING FUNCTION

In general, the phase shift of the compensator $C(s)$ results in a “clipped” ellipse in the τ_a -versus- θ plane. If we define a new torque variable

$$\tau' = \tau_a + \beta_o \dot{\theta} \quad (2-1)$$

then τ' is subject to the simple limiting function $l(\tau + \beta_o \dot{\theta})$ given by

$$\tau' = l(\tau + \beta_o \dot{\theta}) = \begin{cases} \tau + \beta_o \dot{\theta}, & -\tau_o < \tau + \beta_o \dot{\theta} < \tau_o \\ \tau_o, & \tau + \beta_o \dot{\theta} \geq \tau_o \\ -\tau_o, & \tau + \beta_o \dot{\theta} \leq -\tau_o \end{cases} \quad (2-2)$$

Now since the demanded torque τ is related to the joint velocity $\dot{\theta}$ by the transfer function $C(s)/s$, we can represent the behavior of the delivered torque τ_a as a function of the velocity as shown in Figure 2-1.

The describing function of the block diagram in Figure 2-1 can be readily computed. First, the particular form of l results in a describing function which depends on the magnitude of its input only, with no phase shift. Let

$$\lambda = |(C(j\omega)/j\omega + \beta_o)\dot{\theta}(j\omega)| \quad (2-3)$$

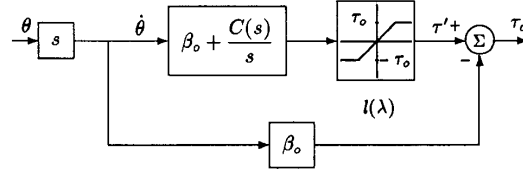


Figure 2-1: Model of the controller/actuator.

represent the magnitude of this input. The limiting describing function $l(\lambda)$ is given by

$$l(\lambda) = 1 - \frac{2\delta}{\pi} - \frac{1}{\pi} \sin(2\delta) + \frac{4}{\pi} (\tau_o/\lambda) \sin(\delta) \quad (2-4)$$

where the parameter δ indicates the degree of actuator non-linearity and is given by

$$\delta = \begin{cases} 0, & \lambda < \tau_o \\ \pi/2 - \sin^{-1}(\tau_o/\lambda), & \lambda \geq \tau_o \end{cases} \quad (2-5)$$

The functions $l(\lambda)$ and $\delta(\lambda)$ are plotted in Figure 2-2. These

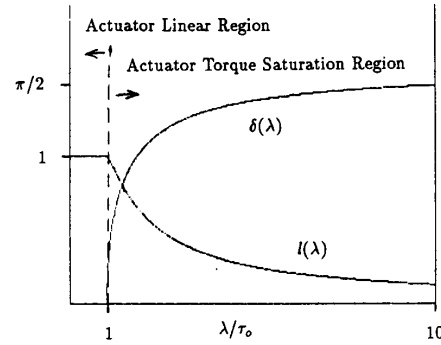


Figure 2-2: Describing function l and linearity parameter δ versus the amplitude factor λ .

curves show the essential effect of the torque/speed non-linearity. When δ is zero, the demanded torque is within the linear region of the torque/speed constraint, and the control action is determined by the linear controller C . When $\delta > 0$, the actuator becomes nonlinear, and l acts to reduce the gain of the feedback control block.

From the block diagram and the describing function l we have

$$D(j\omega) = \frac{\tau_a(j\omega)}{\theta(j\omega)} = j\omega l(\lambda) \cdot [\beta_o + C(j\omega)/j\omega] - j\omega \beta_o. \quad (2-6)$$

This equation fully describes the interdependence of actuator torque/speed constraints and controller dynamics in the manipulator system feedback path.

The next section combines these results with the expression for the closed loop impedance from Section 1 to develop manipulator system design constraints and performance limitations.

3. USE OF THE ACTUATOR DESCRIBING FUNCTION

This section discusses two possible uses of the results of Sections 1 and 2 for preliminary system design or feasibility studies. The first approach is to maintain linear operation through design or operational constraints. The second approach is to evaluate the closed loop performance under actuator saturation, so that the nonlinear behavior can be factored into the design process.

The closed loop system of Section 1 is completely characterized by the achieved impedance Z_c while the system operates in the actuator's linear region. As developed in Section 2, the parameter δ indicates the degree of nonlinearity in the actuator for a particular motion amplitude $|\theta|$. When $\delta = 0$, the system is entirely linear. From (2-5), a suitable linear design strategy would be to require $\lambda < \tau_o$, or using (2-3), to require

$$|\theta(j\omega)| = \left| \frac{\dot{\theta}(j\omega)}{j\omega} \right| < \frac{\tau_o}{|C(j\omega) + j\omega\beta_o|}. \quad (3-1)$$

The magnitude of motion $|\theta(j\omega)|$ is determined by the amplitude of the external torque τ_d , as well as the parameters in the controller C and the manipulator impedance Z_m . For a sinusoidal torque disturbance

$$\tau_d = d \sin(\omega t + \phi) \quad (3-2)$$

the amplitude d and the motion amplitude $|\theta(j\omega)|$ are related by

$$d = |Z_m(j\omega) - C(j\omega)| \cdot |\theta(j\omega)|. \quad (3-3)$$

Combining (3-1), (3-3), and the expression (1-2) for C we arrive at the "keep it linear" design constraint

$$\frac{d}{|Z_c(j\omega)|} < \frac{\tau_o}{|j\omega\beta_o + Z_m(j\omega) - Z_c(j\omega)|}. \quad (3-4)$$

A number of design scenarios could be based on (3-4). Two cases of particular interest are:

1. Control Design: Given a manipulator (given the dynamics in Z_m and the actuator torque/speed parameters τ_o and β_o), the allowed external torque amplitude d can be described as a function of the desired closed loop impedance Z_c . For a particular impedance Z_c , an "envelope" of external torques can be described which yield linear manipulator behavior. Conversely, given a desired envelope of torques, allowed closed loop impedance Z_c can be prescribed. Then the envelope of torques can be translated into an envelope of positions, about the nominal (no environmental contact) position, where linear operation is achieved.
2. Manipulator Design: Given a desired "envelope" of external torques, and the closed loop impedance desired within that envelope (i.e. given d and Z_c), select an actuator/manipulator combination such that τ_o , β_o , and $Z_m(j\omega)$ satisfy (3-4) for all ω , or over some

reasonable range of ω . This would allow trade-offs in mechanical design and actuator technology to be considered early in the control design process.

A second design approach would be to allow nonlinear behavior, but guarantee that acceptable performance is maintained. Using the expression (1-6) for the closed loop impedance, together with the expression (2-6) for the describing function of the controller/actuator, we have the closed loop describing function

$$Z(j\omega) = (1 - l(\lambda)) \cdot (Z_m(j\omega) + j\omega\beta_o) + l(\lambda)Z_c(j\omega) \quad (3-5)$$

relating the sinusoidal motion θ to external torque τ_d . By the definition (2-4) of the limiting function l , it is unity while the system is operating in the linear region, and tends to zero as the amplitude factor λ becomes large. Thus, for small amplitudes $|\theta|$, $Z(j\omega) = Z_c(j\omega)$, and as the motion amplitude becomes large, $Z(j\omega) \rightarrow Z_m(j\omega) + j\omega\beta_o$. When the motion amplitude is large, the behavior of the closed loop system is much like the open loop system, but with increased damping due to β_o . When the motion amplitude is small, the closed loop response matches the linear control design. The function l acts to shift the "weight" of closed loop behavior between these two extremes.

For each frequency, the measure of what is a "large" amplitude is determined with the definition (2-3) of the amplitude factor λ , together with the functional form of $l(\lambda)$ given in Figure 2-2. For example, if the amplitude of θ is twice as large as the linear limit, the closed loop behavior is 61 percent determined by the linear control law, and 39 percent determined by the nonlinear limiting extreme. When the amplitude exceeds the linear limit by a factor of five, the manipulator behavior is mostly (75 percent) like the nonlinear limit, with just 25 percent of the linear control behavior remaining.

A general control design objective is to improve the stiffness of the manipulator to allow for good position control (increase the low frequency impedance), yet reduce the impedance at high frequencies to provide greater mobility or "dexterity". The actuator nonlinearity causes limitations on the achievable impedance, but these restrictions are different for low frequencies than for high frequencies. The gain reduction characteristic of the torque/speed describing function l provides an *upper bound* on the achievable manipulator stiffness, which is a function of the amplitude of the external torque. In contrast, the high frequency impedance is *lower bounded* by the nonlinear behavior, again depending on the external torque amplitude. The overall effect of the torque/speed constraint is to bound the *changes* to the impedance $Z_m(s) + \beta_o s$ possible using feedback control. Since these bounds hold for any controller, it is easy to compare the performance achievable by control design with the performance achievable by mechanical design.

4. EXTENSION TO MULTIPLE DEGREES OF FREEDOM

Compared to the simple analysis of Sections 1-3, additional complication arises in a general manipulator due to the additional degrees of freedom and the nonlinearity of the manipulator kinematics and dynamics. The impedance is now a matrix of scalar impedances of the form derived earlier, each element relating the effort (force or torque) in one coordinate to motion (linear or angular) in another coordinate.

It is usually the cartesian impedance that dictates manipulator behavior in the performance of a task, since the task geometry defines the reference frame the manipulator must ultimately work within. But the actuator nonlinear characteristic is fundamentally a joint space phenomenon, since actuators are usually assigned individually to separate joints. Thus, joint behavior must be translated into cartesian coordinates. The cartesian impedance matrix $Z(j\omega)$ is related to the joint impedance matrix $Z(j\omega)$ by a nonlinear mapping consisting of the kinematic transformation $T(\theta)$ (a nonlinear function of the joint angle vector θ) and its jacobian $J(\theta)$ [1,2]:

$$Z(j\omega) = J^T(\theta)Z(j\omega)T(\theta) \quad (4-1)$$

If the manipulator is kinematically redundant, a unique solution of this equation for $Z(j\omega)$ will not exist. Otherwise, assuming θ is away from a kinematic singularity, we can write

$$Z(j\omega) = J^{-T}(\theta)Z(j\omega)T^{-1}(\theta) \quad (4-2)$$

to describe the manipulator behavior in cartesian space.

In certain special cases [19] the manipulator dynamics may be decoupled and invariant with respect to joint position. In general, however, the dynamics of a multiple joint manipulator take the form [20]

$$T_a + T_d = M(\theta)\ddot{\theta} + S(\theta, \dot{\theta}) + G(\theta) = Z_m(\theta) \quad (4-3)$$

where T_d and T_a are vectors of joint disturbance and actuator torques, respectively, and θ is a vector of joint angles. $M(\theta)$ is the inertia matrix, $S(\theta, \dot{\theta})$ is a vector of centripetal, coriolis, and damping torques, and $G(\theta)$ is a vector of gravity torques. If actuator nonlinearities are not present, the feedback controller is represented by

$$T_a = C(\theta) = Z_m(\theta) - Z_c(\theta) \quad (4-4)$$

and the closed loop impedance is given by

$$T_d = Z_m(\theta) - C(\theta) = Z_c(\theta). \quad (4-5)$$

This impedance is a nonlinear dynamic function due to the manipulator dynamic nonlinearities.

If the actuator torque/speed nonlinearity is included, the controller description C is replaced by the describing function D derived as follows. Let T be the vector of sinusoidal torques demanded by the controller for sinusoidal motions θ . As in Section 2, define the vector of auxiliary torques T' as $T_a + B_o\dot{\theta}$, where T_a is the vector of supplied

actuator torques, and B_o is a diagonal matrix of back EMF constants for each joint. Each element of the torque vector T' is then limited to the corresponding element of the stall torque vector T_o via limiting functions of the form (2-2). The resulting multiple joint version of the actuator/controller given in Section 2 is shown in block diagram form in Figure 4-1. The describing function of the feedback

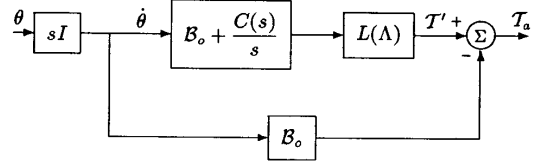


Figure 4-1: Multiple degree of freedom actuator/controller.

controller in the presence of actuator torque/speed limitations is readily computed from this block diagram:

$$D(j\omega) = L(\Lambda)(j\omega B_o + C(j\omega)) - j\omega B_o \quad (4-6)$$

where $L(\Lambda)$ is a diagonal matrix of limiting functions, operating on the vector of amplitude parameters $\Lambda = [\lambda_i]$. Combining the manipulator impedance with the feedback controller/actuator describing function yields the closed loop joint coordinate impedance

$$Z(j\omega) = (I - L(\Lambda)) \cdot [Z_m(\theta) + j\omega B_o] + L(\Lambda) \cdot Z_c(\theta) \quad (4-7)$$

in complete analogy with the simple results of Section 3. In this form, the sinusoidal impedance Z is an accurate description of dynamic behavior, but it is quite complicated due to the form of the open loop impedance Z_m .

In many situations involving contact with objects in the manipulator's workspace, interaction occurs in the neighborhood of a fixed manipulator configuration. That is, joint angles remain in the vicinity of nominal values θ_o throughout the contact encounter. Since the manipulator dynamics, represented by $Z_m(\theta)$, are smooth functions of manipulator joint position, a linearized model

$$Z_m(\theta) = M_o\ddot{\theta} + B_o\dot{\theta} \quad (4-8)$$

can be quite accurate for small sinusoidal motion θ about the nominal joint position θ_o . Here, $M_o = M(\theta_o)$, and $B_o\dot{\theta}$ represents the damping terms in $S(\theta_o, \dot{\theta})$. The corresponding describing function for the manipulator dynamics is then

$$Z_m(j\omega) = -\omega^2 M_o + j\omega B_o. \quad (4-9)$$

Combining the general closed loop impedance formula (4-7) with the simplified manipulator impedance Z_m yields the joint space impedance

$$Z(j\omega) = (I - L(\Lambda)) \cdot [-\omega^2 M_o + j\omega(B_o + B_o)] + L(\Lambda) \cdot Z_c(j\omega) \quad (4-10)$$

This clearly demonstrates the same type of behavior found in the simpler analysis presented earlier. When each of the motion magnitude factors λ_i in Λ are smaller than their respective stall torques $\tau_{o,i}$ in \mathcal{T}_o , then $L(\lambda) = I$, linear operation is retained, and the manipulator impedance is given by $Z_c(j\omega)$. When any joint motion magnitude becomes large enough to cause $\lambda_i > \tau_{o,i}$, then the extreme impedance $-\omega^2 M_o + j\omega(B_o + \mathcal{B}_o)$ is blended with the desired value Z_c according to the limiting functions $l_i(\lambda_i)$, defined in (2-4). This general impedance in joint space can be transformed using (4-2) to describe cartesian interaction with a manipulation task.

CONCLUSION

In the absence of analytical guidelines, robot manipulator system designs have relied on implementation experience. For applications which have used manipulators successfully, such as in factory automation of welding, sealant application, or spray painting, the design process is relatively mature. For new robotics applications, however, such design experience is not available. Particularly where extensive testing is expensive, as in space and undersea applications, is it important to understand the capabilities of a design before it is built. This understanding requires answers to some basic questions: When a particular technology is used, what levels of manipulator performance are possible? Given a desired level of overall manipulator performance, what are the specific requirements on the component parts of the system? Which components are critical factors in the overall performance capability?

This paper has addressed these questions by examining manipulator performance capabilities/limitations due to a specific actuator technology—DC permanent magnet electric motors. It was shown that the closed loop impedance $Z(j\omega)$ is a linear combination of two specific impedances, the open loop impedance plus back EMF damping $Z_m(j\omega) + j\omega\beta_o$, and the designed closed loop impedance Z_c . When the external or disturbance torques are small, the impedance specified by the control design is achieved. As the disturbance torques increase, the open loop impedance plus back EMF damping begins to dominate the overall behavior. The proportions of these two distinct impedances are determined by the limiting describing functions $l_i(\delta_i)$, where δ_i is a measure of the degree of actuator non-linearity for each manipulator joint.

These quantitative results show how the actuator torque/speed capability limits the ability of feedback control to change the open loop manipulator behavior. This allows control design and mechanical design to be integrated together at an early stage in the design process. It also provides basic information about what performance is feasible using this actuator technology.

REFERENCES

- [1] N. Hogan, "Impedance control: an approach to manipulation", *ASME J. Dyn. Sys., Meas., and Control*, June, 1981, pp. 126-133.
- [2] O. Khatib, "A unified approach for motion and force control of manipulators", *IEEE J. Robotics and Automation*, Feb., 1987, pp. 890-896.
- [3] N. Hogan, "Some computational problems simplified by impedance control" *Proc. IEEE Intl. Conf. on Robotics and Automation*, Raleigh, NC, April, 1987, pp. 203-209.
- [4] S. D. Eppinger and W. P. Seering, "Understanding bandwidth limitations in robot force control", *Proc. IEEE Intl. Conf. on Robotics and Automation*, Raleigh, NC, April, 1987, pp. 904-909.
- [5] H. Kazerooni, "Compliant motion control for robot manipulators (input-output approach)", *Proc. IEEE Intl. Conf. on Robotics and Automation*, Raleigh, NC, April, 1987, pp. 812-820.
- [6] T. Stepien, L. Sweet, and M. Good, "Control of tool/workpiece contact force with application to robotic deburring", *Proc. IEEE Intl. Conf. on Robotics and Automation*, St. Louis, MO, 1985, pp. 670-679.
- [7] M. P. Hennessey, J. A. Priebe, P. C. Huang, and R. J. Grommes, "Design of a lightweight robotic arm and controller" *Proc. IEEE Intl. Conf. on Robotics and Automation*, Raleigh, NC, April, 1987, pp. 779-785.
- [8] C. Muller and H. VanLandingham, "A nonlinear feedback controller for an electro-hydraulic robot arm", *Proc. 1985 American Control Conf.*, Boston, MA, June, 1985, pp. 737-740.
- [9] D. A. Lawrence, "Impedance control stability properties in common implementations", *Proc. IEEE Intl. Conf. on Robotics and Automation*, Philadelphia, PA, April, 1988, pp. 1185-1191.
- [10] K. A. Pasch and W. P. Seering, "On the drive systems for high-performance machines", *ASME J. of Mech., Trans., and Automation in Design*, vol. 106, March, 1984, pp. 102-108.
- [11] T. Yoshikawa, "Dynamic manipulability of robot manipulators", *Proc. IEEE Intl. Conf. on Robotics and Automation*, St. Louis, MO, 1985, pp. 1033-1038.
- [12] H. Asada, "A geometrical representation of manipulator dynamics and its application to arm design", *ASME J. of Dyn. Sys., Meas., and Control*, vol. 105, no. 3, 1983, pp. 131-135.
- [13] M. Spong, J. Thorp, and J. Kleinwaks, "The control of robot manipulators with bounded inputs", *Proc. 18th Conf. on Info. Sci. and Sys.*, Princeton, NJ, March, 1984, pp. 685-689.
- [14] J. -J. Slotine, "The design/modeling/performance trade-offs in high-speed robot manipulators", *Proc. 1985 American Control Conf.*, Boston, MA, June, 1985, pp. 710-715.
- [15] H. Merritt, *Hydraulic Control Systems*, John Wiley, 1967.
- [16] K. Lee and D. Tortorelli, "A CAD system for designing robotic manipulators", *Proc. IEEE Intl. Conf. on Robotics and Automation*, St. Louis, MO, 1985, pp. 376-380.
- [17] N. Minorski, *Theory of Non-Linear Control Systems*, McGraw Hill, 1969.
- [18] D. Atherton, *Nonlinear Control Engineering*, Van Nostrand Reinhold, London, 1982.
- [19] K. Youcef-Toumi and H. Asada, "The design of open-loop manipulator arms with decoupled and configuration-invariant inertia tensors", *ASME J. of Dyn. Sys., Meas., and Control*, Vol. 109, Sept., 1987, pp. 268-275.
- [20] R. P. Paul, *Robot Manipulators: Mathematics, Programming, and Control*, The M. I. T Press, 1981.
- [21] J. Vertut and A. Liegeois, "General design criteria for manipulators", *Mechanism and Machine Theory*, vol. 16, 1981, pp. 65-70.